Synthesis of Anthracene End-Capped Poly(methyl methacrylate)s via Atom Transfer Radical Polymerization and Its Kinetic Analyses

Huiqi Zhang,* Bert Klumperman, and Rob van der Linde*

Department of Polymer Chemistry and Coatings Technology, Eindhoven University of Technology, P.O. Box 513, 5600 MB Eindhoven, The Netherlands

Received September 5, 2001

ABSTRACT: The synthesis of anthracene end-capped poly(methyl methacrylate)s via atom transfer radical polymerization (ATRP) and the kinetic analyses thereof are reported. Methyl methacrylate was polymerized in toluene at 90 °C (or 60 °C) via ATRP using 9-anthracenemethyl-2-bromoisobutyrate as the initiator and CuBr/*N*-(*n*-hexyl)pyridylmethanimine as the catalyst. Anthracene end-capped polymers with predetermined molecular weights and low polydispersities (PDI < 1.3) were obtained and characterized by ^{1}H NMR and UV−vis. The initiator and Cu(I) concentrations, initially added Cu(II) concentration, and reaction temperature of the ATRP system have a decisive effect on the kinetics of the reaction. When the initiator and Cu(I) concentrations or the reaction temperature are relatively high, or the initially added Cu(II) concentration is relatively low, and consequently the radical concentration in the system is relatively high, the kinetics of the polymerization fits Fischer's equation ($\ln([M]_0/[M]) \propto t^{2/3}$). On the other hand, Matyjaszewski's equation ($\ln([M]_0/[M]) \propto t$) can be fitted quite well when the initiator and Cu(I) concentrations or the reaction temperature are so low or the initially added Cu(II) concentration becomes so high that radical termination is negligible. This kinetic transition is of great importance for better understanding the mechanism of ATRP. The equilibrium and termination constants (K_{eq} and k_t) for the studied ATRP system at 90 °C are 9.1×10^{-8} and 1.3×10^8 M^{-1} s^{-1}, respectively. The experimental evidence for Fischer's theoretically derived threshold Cu(II) concentration for the kinetic transition, i.e., $[Cu(II)]_{0,t} = (3K_{eq}[RX]_0[Cu(I)]_0k_t/k_p)^{1/2}$, is provided.

Introduction

Anthracene-containing polymers have attracted much attention due to their potential use as semiconductors, photoresist materials, and fluorescent probes.[1−3] Various methods have been developed to attach anthracene moieties to polymers.[1−12] Conventional free radical polymerization is usually used for the synthesis of anthracene-containing polymers since it is easy to perform,[1−8] but the structures of the polymers obtained in this way are ill-defined; i.e., the molecular weights are not predetermined, and the molecular weight distributions are broad. Anionic polymerization has been used to solve this problem, and well-defined anthracene-containing polymers with predetermined molecular weights and low polydispersities were obtained.[9] However, anionic polymerization requires very stringent reaction conditions, which makes it difficult to perform, and the choice of monomers is quite limited.

In recent years, atom transfer radical polymerization (ATRP) has received rapidly increasing interest due to its versatility.[13−16] ATRP is based on a fast, dynamic equilibrium established between the dormant species (alkyl halides) and active species (radicals), with transition-metal complexes acting as reversible halogen atom transfer reagents, which keeps a very low radical concentration (approximately 10^{-7}−10^{-8} M)[17] in the reaction system and thus results in negligible radical termination and controlled polymerization. It not only provides polymers with controlled molecular weights and narrow molecular weight distributions but can also be performed using ordinary radical polymerization procedures for a variety of monomers, avoiding the stringent conditions needed for living ionic polymerization. Many monomers have been successfully polymerized by ATRP, such as styrene, (meth)acrylates, and acrylonitrile, and polymers with low polydispersities and specific functional end groups have been obtained.[15,16]

ATRP and a combination of ATRP with other methods have been used to synthesize anthracene-containing polymers.[10−12] Kim et al. reported the preparation of anthracene-labeled poly(methyl methacrylate)s (PMMAs) via ATRP, where PMMAs bear anthracene units in the middle of the chains, but the initiation efficiency of the polymerization was rather low (<20%), which was presumably due to some side reactions that compete with the initiation reaction.[10] Ohno et al. synthesized well-defined anthracene-labeled polystyrenes via ATRP using 9,10-bis(1-bromoethylcarbalkoxymethyl)anthracene as the bifunctional initiator and CuBr/4,4′-di(*n*-heptyl)-2,2′-bipyridine as the catalyst with an initiation efficiency of 100%.[11] More recently, Tong et al. reported the synthesis of (meth)acrylate-based diblock copolymers bearing an anthracene group at the junction by combining anionic polymerization and ATRP.[12]

This paper reports the synthesis of well-defined anthracene end-capped PMMAs via ATRP using 9-anthracenemethyl-2-bromoisobutyrate (AMBIB) as the initiator and CuBr/*N*-(*n*-hexyl)pyridylmethanimine (NHPMI) as the catalyst. The high initiation efficiency obtained and the well-defined structures of the obtained polymers indicate that the experimental system is free of significant side reactions and is thus quite suitable for kinetic studies. Therefore, the kinetics of the system was also studied to continue our effort in understanding the mechanistic aspect of the ATRP system. Two well-known equations have been proposed to describe the kinetics of the ATRP system by Matyjaszewski (eq 1)[18] and by Fischer (eq 2).[19]

---

* Corresponding authors: Fax 31-40-2463966; e-mail Zhanghuiqi@hotmail.com and R.van.der.Linde@tue.nl.

10.1021/ma011575z CCC: $22.00

$$\ln\left(\frac{[\mathrm{M}]_0}{[\mathrm{M}]}\right) = k_\mathrm{p}K_\mathrm{eq}\frac{[\mathrm{RX}][\mathrm{Cu(I)}]}{[\mathrm{Cu(II)}]}\,t = k_\mathrm{p}[\mathrm{R}^\bullet]t = K_\mathrm{app}t \quad \text{(M-Eq)} \quad (1)$$

$$\ln\left(\frac{[\mathrm{M}]_0}{[\mathrm{M}]}\right) = \frac{3}{2}k_\mathrm{p}([\mathrm{RX}]_0[\mathrm{Cu(I)}]_0)^{1/3}\left(\frac{K_\mathrm{eq}}{3k_\mathrm{t}}\right)^{1/3}t^{2/3} = K_\mathrm{Fischer}t^{2/3} \quad \text{(F-Eq)} \quad (2)$$

A third equation was derived by Snijder et al. for the specific system where Cu(II) has a limited solubility in the reaction mixture.[20] Since the presently studied system is homogeneous, the equation by Snijder et al. will not be considered here. Matyjaszewski's equation (eq 1, M-Eq) has been used in almost all kinetic studies of the ATRP,[18,21−25] and only recently has Fischer's equation (eq 2, F-Eq) proven to be applicable in the ATRP system.[26] The present work further explores the kinetics of the ATRP by using a combination of M-Eq and F-Eq and presents the effects of the initiator and Cu(I) concentrations, initially added Cu(II) concentration, and reaction temperature of the ATRP system on the kinetics of the polymerization.

Experimental Section

Materials. Methyl methacrylate (MMA) (Aldrich, 99%) was washed twice with an aqueous solution of sodium hydroxide (5%) and twice with distilled water, dried with anhydrous magnesium sulfate overnight, and then distilled over calcium hydride under vacuum. The distillate was stored at −18 °C before use. Toluene (Biosolve Ltd., AR) was distilled over calcium hydride. CuBr (Aldrich, 98%) was stirred with acetic acid for 12 h, washed with ethanol and diethyl ether, and then dried under vacuum at 75 °C for 3 days. The purified CuBr was stored in an argon atmosphere. Dichloromethane (Biosolve Ltd., HPLC) was dried with calcium hydride and then distilled. NHPMI was synthesized by condensation of pyridine-2-carboxaldehyde (Acros, 99%) and *n*-hexylamine (Acros, 99%) as described elsewhere.[21] $\mathrm{CuBr_2}$ (Aldrich, 99%), 9-anthracenemethanol (Aldrich, 97%), 2-bromoisobutyryl bromide (Aldrich, 98%), aluminum oxide (activated, basic, for column chromatography, 50−200 μm), and all the other chemicals were used as received.

Synthesis of AMBIB. Triethylamine (2.633 g, 26.02 mmol) was added to a solution of 9-anthracenemethanol (4.166 g, 20.00 mmol) in dry dichloromethane (90 mL). The solution was stirred in an ice bath, and 2-bromoisobutyryl bromide (5.985 g, 26.03 mmol) in dry dichloromethane (10 mL) was added dropwise over a period of 0.5 h. The reaction mixture was stirred at 0 °C for 1 h and then at 25 °C overnight. The solution was filtered, washed three times with an aqueous solution of hydrochloride (0.5 M), and then washed three times with distilled water. Finally, the solution was dried with anhydrous magnesium sulfate overnight, and the solvent was removed under vacuum. The obtained crude product was purified by recrystallization three times from methanol to give a pale yellow solid (5.1 g, 72%); mp 84−85 °C. UV−vis (chloroform): λ_max/nm (ϵ/L mol^{-1} cm^{-1}) = 334 (2971), 350 (5919), 368 (8792), 388 (8117). ^{1}H NMR ($\mathrm{CDCl_3}$): δ = 8.53 (s, 1H, Ar−H (10)), 8.36−8.34 (m, 2H, Ar−H (1,8)), 8.06−8.03 (m, 2H, Ar−H (4,5)), 7.61−7.48 (m, 4H, Ar−H (2,3,6,7)), 6.23 (s, 2H, $\mathrm{CH_2}$), 1.88 (s, 6H, $\mathrm{CH_3}$).[27] ^{13}C NMR ($\mathrm{CDCl_3}$): δ = 172.00 (COO), 131.45 (Ar−C (9)), 131.22 (Ar−C (8a,9a)), 129.51 (Ar−C (4,5)), 129.19 (Ar−C (1,8)), 126.81 (Ar−C (10)), 125.62 (Ar−C (2,7)), 125.22 (Ar−C (3,6)), 123.99 (Ar−C (4a,10a)), 60.80 ($\mathrm{CH_2}$), 56.03 (C−Br), 30.81 ($\mathrm{CH_3}$).[27] MS: m/z = 358.0 ([M + H]$^+$, calcd for $\mathrm{C_{19}H_{18}O_2Br}$ 358.2).

Polymerization Procedure. A typical ATRP was carried out as follows. CuBr (0.270 g, 1.88 mmol) and NHPMI (0.818 g, 4.30 mmol) were added to a solution of MMA (9.459 g, 94.48 mmol) and toluene (17.360 g) in a three-neck round-bottom flask (100 mL). After the reaction mixture was bubbled with argon for 30 min in an ice bath, the initiator AMBIB (0.669 g, 1.87 mmol) was added. The solution was bubbled with argon again for 20 min in an ice bath. The flask was then immersed in a thermostated oil bath at 90 °C and stirred. The polymerization was sampled at suitable time periods throughout the reaction. The sample was diluted with tetrahydrofuran (THF), and part of it was used for gas chromatography (GC) measurements to determine monomer conversion. The rest was passed through a column of basic aluminum oxide prior to size exclusion chromatography (SEC) measurements. After 6 h, the reaction was quenched by cooling the solution. The reaction mixture was passed through a column of basic aluminum oxide to remove the catalyst, part of the solvent was evaporated, and the rest was precipitated into methanol. After washing three times with methanol, the filtered product was dried at 50 °C under vacuum for 3 days to give polymer I in 89% yield.

Measurements. The melting point of the initiator was determined by a melting point measuring apparatus named after Dr. Tottoli (W. Büchi Glass Apparatus Factory, Flawil, Switzerland). ^{1}H NMR and ^{13}C NMR spectra were recorded on Varian-300 and Varian-400 spectrometers using TMS as an internal standard. Gas chromatography−mass spectroscopy (GC-MS) measurement was performed on a GC-MS QP-5000 (Shimadzu). Monomer conversion was determined from the concentration of residual monomer using a Hewlett-Packard 5890 GC, equipped with AT-Wax capillary column (30 m × 0.53 mm × 10 μm) using toluene as an internal reference. Molecular weights and molecular weight distributions were measured by SEC using a Waters GPC equipped with a Waters model 510 pump and a model 410 differential refractometer (40 °C). THF was used as eluent at a flow rate of 1.0 mL/min. A set of two linear columns (Mixed-C, Polymer Laboratories, 30 cm, 40 °C) was used. The calibration curve was prepared with polystyrene (PS) standards, and molecular weights were recalculated using the universal calibration principle and Mark−Houwink parameters (PS: $K = 1.14 \times 10^{-4}$ dL g^{-1}, $a = 0.716$; PMMA: $K = 0.944 \times 10^{-4}$ dL g^{-1}, $a = 0.719$). UV−vis spectra were recorded on a Hewlett-Packard 8453 UV−vis spectrophotometer. The calibration curve was obtained by plotting absorbance vs concentration for solutions of AMBIB in chloroform. With these values, we could either assess the degree of anthracene incorporation or, assuming complete incorporation, calculate $M_\mathrm{n,UV}$ (number-average molecular weights determined by UV−vis method) for the samples. Glass transition temperatures (T_g) were measured with a Perkin-Elmer Pyris 1 differential scanning calorimeter (DSC) using a heating rate of 10 °C/min. All samples were scanned twice in order to eliminate the thermal history, and the results from the second scan are reported. Glass transition temperatures were read as the midpoint of the change in heat capacity.

Results and Discussion

Degree of Control of the ATRP System. The new anthracene-containing initiator, AMBIB (Scheme 1), was synthesized by reacting 9-anthracenemethanol with 2-bromoisobutyryl bromide and then purified by recrystallization from methanol. Its purity was confirmed by thin-layer chromatography (TLC), ^{1}H NMR, ^{13}C NMR, and GC-MS. AMBIB is soluble in toluene, chloroform, and THF. MMA was polymerized in toluene at 90 °C (or 60 °C) via ATRP using AMBIB as the initiator and CuBr/NHPMI as the catalyst ($\mathrm{CuBr_2}$ was added if necessary) (Scheme 1). The volume of toluene used was always twice that of MMA in each ATRP system, and the molar ratio of AMBIB to CuBr to NHPMI was always 1:1:2.3. A homogeneous dark brown solution was obtained when the reaction mixture was heated to 90 °C (or 60 °C).

Figure 1 shows that the number-average molecular weights of the polymers determined by SEC, $M_\mathrm{n,SEC}$, increase linearly with increasing monomer conversion

Scheme 1

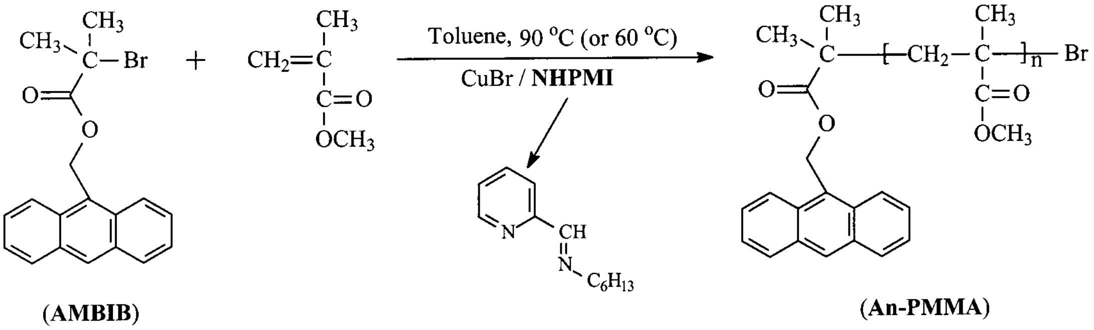

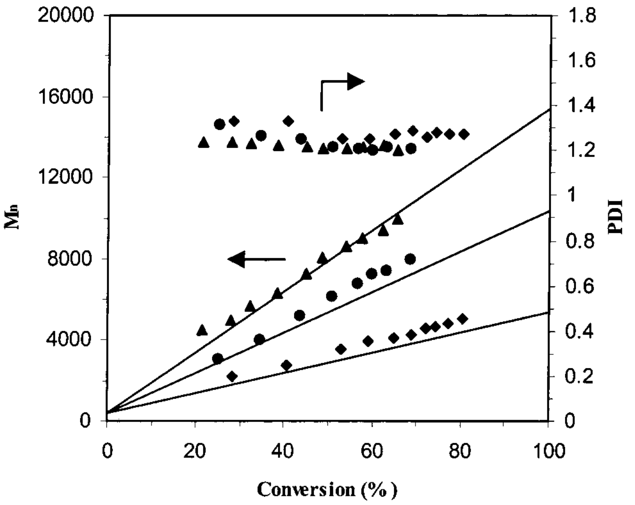

Figure 1. Dependence of $M_{n,SEC}$ and PDI on monomer conversion for the ATRP of MMA in toluene at 90 °C. $[MMA]_0/[AMBIB]_0/[CuBr]_0/[NHPMI]_0 = 50/1/1/2.3$ (◆), 100/1/1/2.3 (●), and 150/1/1/2.3 (▲). Lines represent the theoretical molecular weights ($M_{n,th}$).

and are quite close to the theoretical values determined by $M_{n,th} = ([M]_0/[RX]_0)M_MC + M_{RX}$, where $[M]_0$ and $[RX]_0$ are the initial concentrations of monomer and initiator, respectively, M_M and M_{RX} are the molecular weights of monomer and initiator, respectively, and C is the monomer conversion. This, together with the low polydispersity indices (PDI) of the polymers (<1.3 in most cases), suggests that the polymerization is living and well-controlled. The initiation efficiency of the polymerization, i.e., $M_{n,th}/M_{n,SEC}$, was calculated to be 88%, 90%, and 96% for the ATRP systems with reactant ratio $\varphi = [MMA]_0/[AMBIB]_0/[CuBr]_0/[NHPMI]_0$ of 50/1/1/2.3, 100/1/1/2.3, and 150/1/1/2.3 at a reaction time of 6 h, respectively,[28] indicating that the polymerization is better controlled at lower initiator and Cu(I) concentrations, just as discussed later (see the kinetic analyses section). The high initiation efficiency obtained demonstrates that side reactions are quite limited in the polymerization process. Note that the radical polymerization of acrylates and styrene in the presence of anthracene or its derivatives is usually perturbed by the competing radical addition to the 9- and/or 10-position of the anthracene. Methacrylate monomers, however, do not show these side reactions in the presence of anthracene or its derivatives.[12,29,30]

Polymer Characterization. Three polymers, namely polymers I, II, and III, were prepared using different reactant ratios φ in the ATRP system (Table 1). TLC analyses showed that all of them are pure and free of unreacted AMBIB. The strong blue fluorescence observed for all these polymers under a 350 nm UV lamp, therefore, indicates that the anthracene moiety has been chemically incorporated into the polymers. The $M_{n,SEC}$ and PDI for polymers I–III are listed in Table 1.

Figure 2 (parts a and b) shows the ^{1}H NMR spectra of AMBIB and polymer I. The typical proton signals of the anthracene moiety in Figure 2a are also seen in the spectrum of the polymer (6.0–8.6 ppm, Figure 2b), suggesting that the anthracene moiety has been successfully attached to the polymer. Compared with the single peak of the proton signal in $-CH_2-$ connected to the anthracene group of AMBIB at 6.23 ppm (Figure 2a), the multiple splitting of the proton signal of the same group in the polymer at 6.1 ppm further indicates that the anthracene moiety is chemically bonded to the polymer. Furthermore, the number-average molecular weights calculated by comparison of the integration values of the aromatic protons in anthracene and the protons in $-COOCH_3$ of the MMA units ($M_{n,NMR}$) were determined to be 5380, 8020, and 10 700 for polymers I, II, and III, respectively (Table 1), which agree quite well with $M_{n,SEC}$. This confirms that the polymer chains are quantitatively functionalized to generate the desired anthracene end-capped PMMAs.

The UV–vis spectra of the anthracene end-capped PMMAs in chloroform are identical with that of AMBIB in both the shape and peak positions (334, 350, 368, 388 nm) (Figure 3), indicating that anthracene units are definitely present in the polymers and that the ATRP of MMA was not perturbed by the anthracene unit in AMBIB, which is consistent with the previous report.[12] By assuming that the molar extinction coefficient (ϵ) of the polymer-attached anthracene unit is the same as that of AMBIB and that there is only one anthracene group per polymer chain, the number-average molecular weights of the polymers can be calculated by comparing the UV–vis absorbance of the polymer solutions with that of AMBIB, i.e., UV–vis calibration curve of AMBIB. The number-average molecular weights obtained in this way, namely $M_{n,UV}$, agree well with $M_{n,SEC}$ and $M_{n,NMR}$ (Table 1), suggesting that the above assumptions are reasonable, and the anthracene moiety has further proven to be incorporated into the polymers quantitatively.

The glass transition temperature of the polymer increases with increasing molecular weight, as expected (Table 1).

On the basis of the limited side reactions during the ATRP process and the well-defined structures of the obtained polymers as shown above, we conclude that the studied ATRP system is well-controlled and is thus quite suitable for kinetic and mechanistic studies.

Table 1. Number-Average Molecular Weights Determined by SEC, ^{1}H NMR, and UV−vis, Polydispersity Indices, and Glass Transition Temperatures of the Anthracene End-Capped PMMAs

polymer[a]	reactant ratio[b]	reaction temp (°C)	reaction time (h)	$M_{n,SEC}$ (PDI)	$M_{n,NMR}$[c]	$M_{n,UV}$[c]	T_g (°C)
I	50/1/1/2.3	90	6	5790 (1.19)	5380	5240	103
II	100/1/1/2.3	90	6	9100 (1.11)	8020	8610	105
III	150/1/1/2.3	90	10	11500 (1.11)	10700	11100	109

[a] Polymers I, II, and III were prepared via the ATRP of MMA in toluene using AMBIB as the initiator and CuBr/NHPMI as the catalyst and then purified by precipitation into methanol. [b] $[MMA]_0/[AMBIB]_0/[CuBr]_0/[NHPMI]_0$. [c] $M_{n,NMR}$ and $M_{n,UV}$ are calculated by assuming that only one anthracene group is incorporated into each polymer chain.

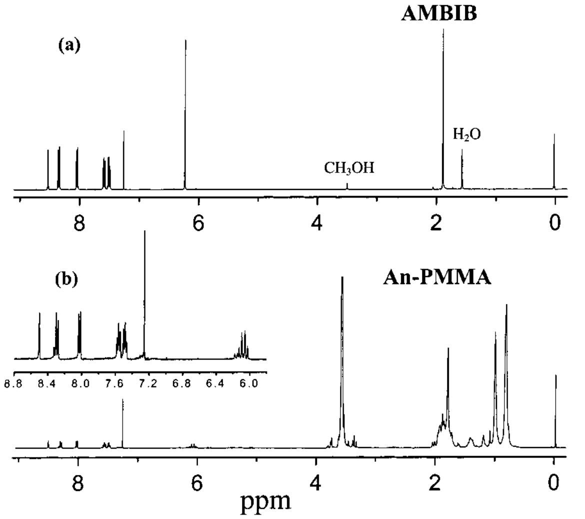

Figure 2. ^{1}H NMR spectra of AMBIB (a) and polymer I (b) in $CDCl_3$.

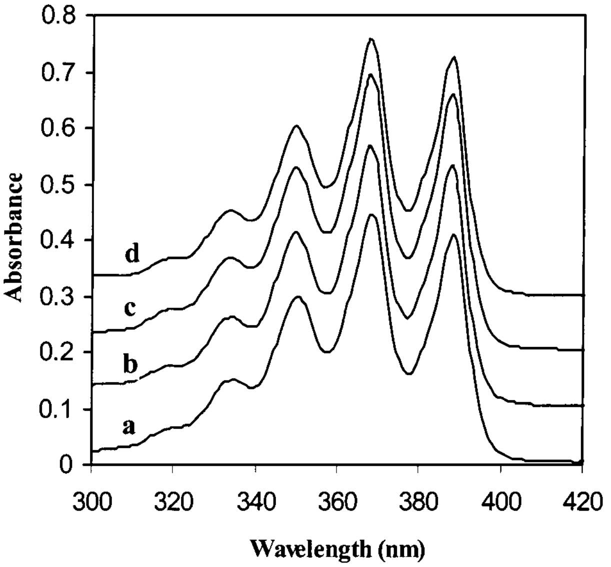

Figure 3. UV−vis spectra of AMBIB and anthracene end-capped PMMAs in chloroform: (a) AMBIB (0.018 mg/mL = 4.99 × 10^{-5} M), (b) polymer I (0.294 mg/mL), (c) polymer II (0.456 mg/mL), (d) polymer III (0.573 mg/mL).

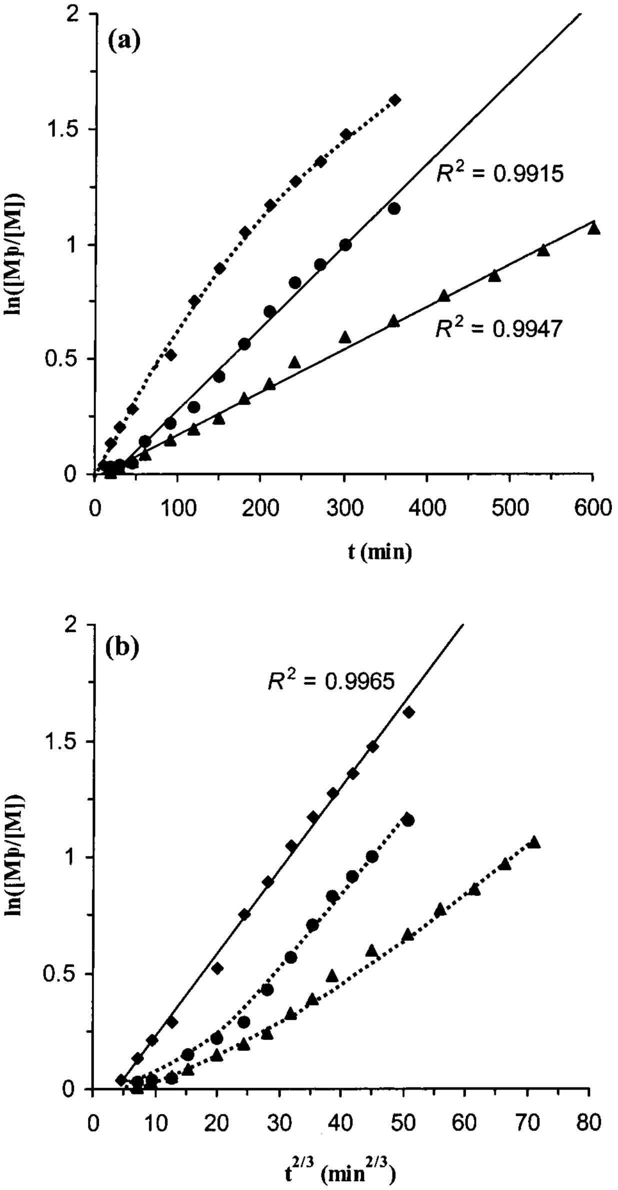

Figure 4. Plots of $\ln([M]_0/[M])$ vs reaction time (t and $t^{2/3}$) for the ATRP of MMA in toluene at 90 °C. $[MMA]_0/[AMBIB]_0/[CuBr]_0/[NHPMI]_0$ = 50/1/1/2.3 (◆), 100/1/1/2.3 (●), and 150/1/1/2.3 (▲).

Effect of Initiator and Cu(I) Concentrations on Kinetics. A series of reactions at different ratios of monomer to initiator and Cu(I) ($[\text{initiator}]_0 = [\text{Cu(I)}]_0$) were carried out at 90 °C to investigate the effect of the initiator and Cu(I) concentrations on the kinetics of the ATRP. The results are shown in Figure 4 (parts a and b). When M-Eq was used to fit the data points of the ATRP systems with reactant ratio φ of 100/1/1/2.3 and 150/1/1/2.3, straight lines with linearity regression coefficients (R^2) greater than 0.99 were obtained. However, the kinetics of the ATRP system with a reactant ratio φ of 50/1/1/2.3 deviates from M-Eq, as demonstrated by a curve (Figure 4a). If we plot $\ln([M]_0/[M])$ against $t^{2/3}$ for this system, however, a straight line with $R^2 = 0.9965$ is obtained (Figure 4b), indicating that this system can be better described by F-Eq. This may be attributed to the radical concentration change following the change of the reactant ratio in the ATRP systems. The radical concentration is relatively high for the ATRP system with a reactant ratio φ of 50/1/1/2.3 due to the relatively high initiator and Cu(I) concentrations, which will lead to some radical termination during the polymerization process. This is consistent with the persistent radical effect; i.e., because of bimolecular radical termination, a Cu(II) level is built up which controls the deactivation reaction.[31] Therefore, M-Eq is inappropriate for this case since it is based on an assumption that radical termination can be neglected. On the contrary, the prerequisite of F-Eq (i.e., radical termination exists) could be met. When the concentrations of initiator and CuBr decrease to such an extent, as in the ATRP systems with reactant ratio φ of 100/1/1/2.3 and 150/1/1/2.3 (the radical concentrations of these two systems were determined to be 3.7×10^{-8} and 1.9×10^{-8} M, respectively, on the basis of M-Eq and the propagation rate constant of MMA, i.e., $k_p = 1625$ M^{-1} s^{-1} at 90 °C[32]), that the radical concentration will be low enough to ensure negligible radical termination, M-Eq describes the kinetics better than F-Eq (Figure 4a,b). The initiator and Cu(I) concentrations in ATRP systems thus have a decisive effect on the kinetics of the polymerization, and the kinetics of the ATRP system switches from fitting F-Eq to fitting M-Eq following the decrease of the initiator and Cu(I) concentrations. The effects of the initiator and Cu(I) concentrations on the kinetics of the ATRP systems have been extensively investigated.[21–26,33,34] However, to the best of our knowledge, no kinetic transition has been found following the change of the initiator and Cu(I) concentrations. This may be due to the reaction conditions selected in the previous studies, including different monomers, ligands, and reactant ratios. In addition, the ATRP systems with reactant ratio φ of 100/1/1/2.3 and 150/1/1/2.3 have an induction period of about 20 min. The cause of this induction period is not very clear yet, and further investigation is going on.

Effect of Initially Added Cu(II) Concentration on Kinetics. $CuBr_2$ was added at the beginning of the reaction to study its effect on the kinetics of the ATRP system, where $[MMA]_0/[AMBIB]_0/[CuBr]_0 = 50/1/1$ and $[CuBr]_0 + [CuBr_2]_0 = [NHPMI]_0/2.3$. Figure 5 shows the kinetic plots of the ATRP systems with different amounts of initially added Cu(II). When the initially added Cu(II) concentration relative to Cu(I) is lower than 15% (i.e., $[Cu(II)]_0/[Cu(I)]_0 < 0.15$), the kinetics of the system is better described by F-Eq. On the other hand, when $[Cu(II)]_0/[Cu(I)]_0 > 0.15$, the kinetics fits M-Eq better than F-Eq. This can also be explained in terms of the radical concentration change following the addition of Cu(II) at the beginning of the polymerization.

Figure 5 also shows that the kinetic transition from fitting F-Eq to fitting M-Eq occurs at a Cu(II) concentration relative to Cu(I) of 15%, where the kinetics of the system can be equally well fitted by both M-Eq and F-Eq (i.e., both fitted lines have linear regression coefficients greater than 0.99). This implies that a concentration of 15% Cu(II) relative to Cu(I) is a threshold level for the switch between the two kinetic regimes. This threshold level is higher than that of the MMA/HEBIB/CuBr/NHPMI system, where HEBIB is 2-hydroxyethyl-2-bromoisobutyrate and the threshold level of Cu(II) is approximately 10% relative to Cu(I), even at higher initiator and Cu(I) concentrations (i.e., $[MMA]_0/[HEBIB]_0/[CuBr]_0/[NHPMI]_0 = 30/1/1/3$).[26] The discrepancy may stem from the different initiators used, which are likely to influence the equilibrium constants K_{eq} and the radical concentrations of the systems. As shown in Figure 5, the induction period appears to depend on the initially added Cu(II) concentration, and its origin is still under investigation.

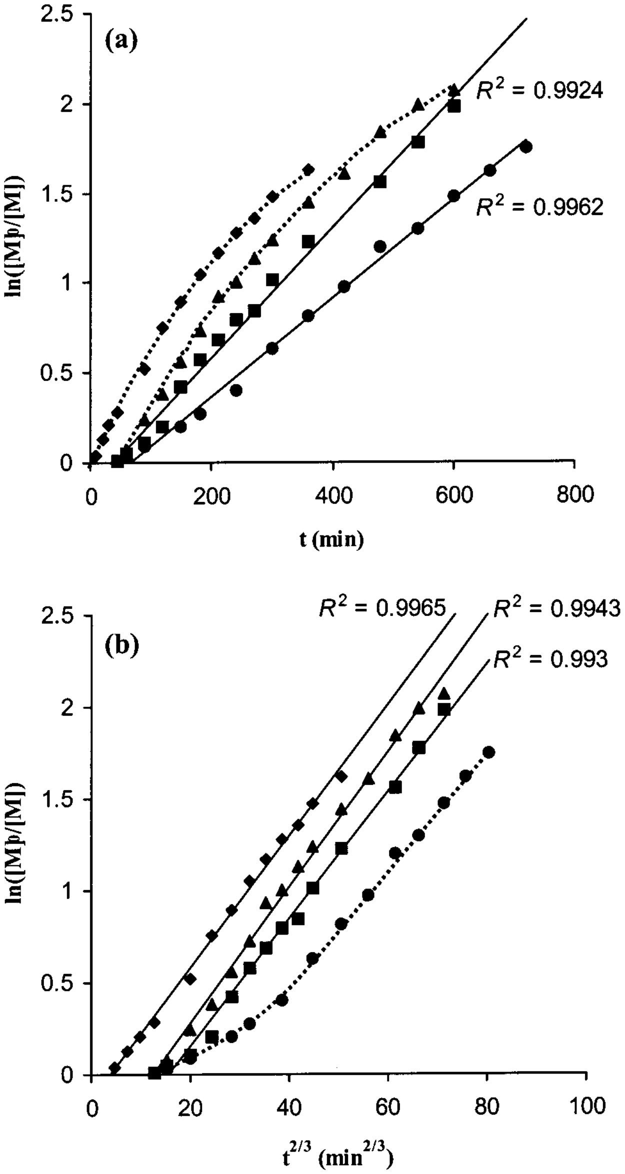

Figure 5. Plots of $\ln([M]_0/[M])$ vs reaction time (t and $t^{2/3}$) for the ATRP of MMA in toluene at 90 °C using different amounts of initially added $CuBr_2$. $[MMA]_0 = 3.0439$ M, $[AMBIB]_0 = [CuBr]_0 = 0.0609$ M, $[CuBr]_0 + [CuBr_2]_0 = [NHPMI]_0/2.3$. $[CuBr_2]_0/[CuBr]_0 = 0$ (◆), 0.11 (▲), 0.15 (■), and 0.2 (●).

The almost equal slopes of the kinetic plots for the ATRP systems with $[Cu(II)]_0/[Cu(I)]_0 = 0$, 0.11, and 0.15 (i.e., slope = 0.0023, 0.0024, and 0.0023 $s^{-2/3}$, respectively) indicate that the polymerization is almost independent of the initially added Cu(II) concentration when $[Cu(II)]_0/[Cu(I)]_0 \leq 0.15$ (Figure 5b). This means that the same amount of Cu(II), i.e., 15% Cu(II) relative to Cu(I), is present in the ATRP systems after the “self-regulation” process at the beginning of the reaction. According to M-Eq, the polymerization rate is inverse first order with respect to the steady-state Cu(II) concentration. Therefore, if we assume that the steady-state Cu(II) concentration is close to the initially added Cu(II) concentration when $[Cu(II)]_0/[Cu(I)]_0 \geq 0.15$, i.e., little self-regulation and radical termination take place in the reaction, the ratio of the slopes of the kinetic plots for the ATRP systems with $[Cu(II)]_0/[Cu(I)]_0 = 0.15$ and 0.20 should be 1.33 on the basis of M-Eq, which is in excellent agreement with the experimental result (1.33) (Figure 5a), demonstrating that our assumptions are reasonable and that the self-regulation process due to bimolecular radical termination in ATRP can be minimized when enough Cu(II) is added at the beginning of the reaction. This result provides direct evidence for the existence of the self-regulation process caused by the persistent radical effect in the ATRP system and a method to minimize it. In addition, the calculated concentrations of propagating radicals for the ATRP systems with $[Cu(II)]_0/[Cu(I)]_0 = 0.15$ and 0.20 are sufficiently low (3.7×10^{-8} and 2.8×10^{-8} M, respectively, based on M-Eq and the k_p of MMA at 90 °C[32]) to prevent significant chain terminations, which is consistent with the above discussion.

The equilibrium constant K_{eq} and termination constant k_t of the studied ATRP system can be derived from Figure 5 (parts a and b). When $[Cu(II)]_0/[Cu(I)]_0 \geq 0.15$, the kinetics of the ATRP system fits M-Eq (Figure 5a), and the steady-state concentrations of initiator, Cu(I), and Cu(II) will be close to their initial concentrations (i.e., $[RX] \approx [RX]_0$, $[Cu(I)] \approx [Cu(I)]_0$, and $[Cu(II)] \approx [Cu(II)]_0$). Therefore, M-Eq can be rewritten to eq 3 in this case.

$$\ln\left(\frac{[M]_0}{[M]}\right) = k_p K_{eq} \frac{[RX]_0[Cu(I)]_0}{[Cu(II)]_0} t = K_{app} t \qquad (3)$$

On the basis of eq 3 and the propagation rate constant of MMA ($k_p = 1625$ M^{-1} s^{-1} at 90 °C),[32] a K_{eq} of 9.1×10^{-8} is derived from the slopes of the straight lines in Figure 5a. Using F-Eq, k_p, and the obtained K_{eq}, we can also obtain a k_t of 1.3×10^8 M^{-1} s^{-1} from the average slope of the straight lines in Figure 5b. These results are reasonable compared with the kinetic data reported elsewhere.[22,26,35]

Recently, Fischer et al. proposed that the transition from nonlinear behavior to linear behavior for the kinetic plots of ATRP systems (i.e., the plots of $\ln([M]_0/[M])$ vs reaction time t) should occur at a theoretical threshold initial Cu(II) concentration of $[Cu(II)]_{0,t} = (3K_{eq}[RX]_0[Cu(I)]_0 k_t/k_p)^{1/2}$,[36] which corresponds to a $[Cu(II)]_{0,t}$ of 0.0090 M in our ATRP system. This value agrees well with the experimental result ($[Cu(II)]_{threshold} = 0.0092$ M).

Effect of Reaction Temperature on Kinetics. Figure 6 shows the effect of reaction temperature on the kinetics of the ATRP system with a reactant ratio φ of 50/1/1/2.3. Since higher temperature enhances the reactivity of polymeric halides toward Cu(I) species, resulting in higher concentration of radicals,[37] the kinetics of ATRP should depend on the reaction temperature. When the polymerization was carried out at 90 °C, the radical concentration in the system was so high that radical termination took place. Therefore, F-Eq described the kinetics better than M-Eq in this case (Figures 4b and 6). On the other hand, when the reaction temperature decreased to 60 °C, the radical concentration in the ATRP system became so low (2.4×10^{-8} M based on M-Eq and a k_p of 834 M^{-1} s^{-1} for MMA at 60 °C[32]) that radical termination was negligible. Accordingly, the system was described well by M-Eq (Figure 6).

Haddleton et al. also studied the effect of the reaction temperature on the kinetics of the ATRP of MMA in toluene (the weight ratio of MMA to toluene is 1 to 3) using ethyl 2-bromoisobutyrate (EBIB) as the initiator and CuBr/*N*-(*n*-pentyl)pyridylmethanimine (NPPMI) as the catalyst with a reactant ratio $[MMA]_0/[EBIB]_0/[CuBr]_0/[NPPMI]_0$ of 100/1/1/3 and found that all the kinetics follow M-Eq, and no kinetic transition occurs when the reaction temperature changes from 90 to 15 °C.[38] This is understandable because their system was even more dilute than our system with a reactant ratio $\varphi = [MMA]_0/[AMBIB]_0/[CuBr]_0/[NHPMI]_0$ of 100/1/1/2.3 (the volume ratio of MMA to toluene is 1 to 2 and the corresponding weight ratio is 1 to 1.85), which fits M-Eq at 90 °C (Figure 4).

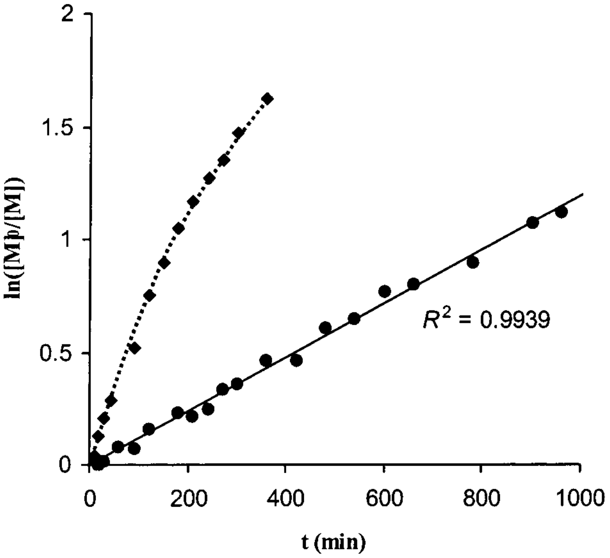

Figure 6. Kinetic plots for the ATRP of MMA in toluene at 60 °C (●) and 90 °C (◆), respectively. $[MMA]_0 = 3.0439$ M, $[AMBIB]_0 = [CuBr]_0 = [NHPMI]_0/2.3 = 0.0609$ M.

According to the above discussion, we conclude that F-Eq should be applicable in the ATRP systems where no side reactions take place except radical termination, and the rate constants are independent of the chain length. M-Eq will be applicable as long as the radical concentration in the ATRP system becomes so low that radical termination can be neglected no matter which of the following three methods, i.e., reducing the concentrations of initiator and/or Cu(I), adding enough Cu(II) at the beginning of the polymerization, or lowering the reaction temperature, is used.

Conclusions

Well-defined anthracene end-capped PMMAs were synthesized via homogeneous ATRP in toluene at 90 °C using AMBIB as the initiator and CuBr/NHPMI as the catalyst. ^{1}H NMR and UV−vis spectroscopy characterizations showed that anthracene units were attached to the polymer chain ends quantitatively (one anthracene group per PMMA chain). The experimental molecular weights of the polymers increase linearly with increasing monomer conversion and are very close to the theoretical values. This, together with the narrow molecular weight distributions (PDI < 1.3), indicates that the polymerization is living and well-controlled. The kinetic studies showed that the initiator and Cu(I) concentrations, initially added Cu(II) concentration, and reaction temperature of the ATRP system can greatly affect the kinetics of the polymerization process. When the reaction proceeds at relatively high initiator and Cu(I) concentrations or at a relatively high reaction temperature, or at a relatively low initially added Cu(II) concentration, the radical concentration in the system is relatively high. In that case the kinetics of the polymerization can be better described by F-Eq ($\ln([M]_0/[M]) \propto t^{2/3}$) due to the presence of radical termination. On the other hand, when the initiator and Cu(I) concentrations or the reaction temperature are so low or the initially added Cu(II) concentration becomes so high that radical termination is negligible, the kinetics of the polymerization switches to fit M-Eq ($\ln([M]_0/[M]) \propto t$). The equilibrium constant K_{eq} and termination constant k_t for the studied ATRP system at 90 °C are 9.1×10^{-8} and 1.3×10^8 M^{-1} s^{-1}, respectively. Fischer's theoretically derived threshold Cu(II) concentration for the kinetic transition from F-Eq to M-Eq, i.e., $[\mathrm{Cu(II)}]_{0,t} = (3K_{eq}[\mathrm{RX}]_0[\mathrm{Cu(I)}]_0 k_t/k_p)^{1/2}$, was experimentally verified.

Acknowledgment. We thank DSM Resins and Senter for financial support, Dr. Ir. Martijn M. G. Antonisse (DSM Resins), Mr. John Rietberg (DSM Resins), and Dr. Weihua Ming for inspiring discussions. We also thank Mr. Wieb Kingma and Mr. Joost L. J. van Dongen for carrying out SEC and GC-MS analyses, respectively.

References and Notes

(1) Anufrieva, E. V.; Gotlib, Y. Y. *Adv. Polym. Sci.* **1981**, *40*, 1.
(2) Takeuchi, K.; Hanaoka, T.; Arakawa, H.; Matsuzaki, T.; Sugi, Y. *Makromol. Chem., Rapid Commun.* **1989**, *10*, 645 and references therein.
(3) Zhang, H.; Verboom, W.; Reinhoudt, D. N. *Tetrahedron Lett.* **2001**, *42*, 4413.
(4) Katz, D. *J. Polym. Sci., Part A* **1963**, *1*, 1635.
(5) Krakovyak, M. G.; Anufrieva, E. V.; Shelekhov, N. S.; Skorokhodov, S. S. *Eur. Polym. J.* **1974**, *10*, 685.
(6) Zhao, C. L.; Wang, Y.; Hruska, Z.; Winnik, M. A. *Macromolecules* **1990**, *23*, 4082.
(7) Tiera, M. J.; De Oliveira, V. A.; Burrows, H. D.; De Graca Miguel, M.; Neumann, M. G. *Colloid Polym. Sci.* **1998**, *276*, 206.
(8) Liu, R.; Winnik, M. A.; Di Stefano, F.; Vanketessan, J. *J. Polym. Sci., Part A: Polym. Chem.* **2001**, *39*, 1495.
(9) Valeur, B.; Monnerie, L. *J. Polym. Sci., Part B: Polym. Phys.* **1976**, *14*, 11.
(10) Kim, C. S.; Oh, S. M.; Kim, S.; Cho, C. C. *Macromol. Rapid Commun.* **1998**, *19*, 191.
(11) Ohno, K.; Fujimoto, K.; Tsujii, Y.; Fukuda, T. *Polymer* **1999**, *40*, 759.
(12) Tong, J. D.; Zhou, C.; Ni, S.; Winnik, M. A. *Macromolecules* **2001**, *34*, 696.
(13) Wang, J. S.; Matyjaszewski, K. *J. Am. Chem. Soc.* **1995**, *117*, 5614; *Macromolecules* **1995**, *28*, 7901.
(14) Kato, M.; Kamigaito, M.; Sawamoto, M.; Higashimura, T. *Macromolecules* **1995**, *28*, 1721.
(15) Patten, T.; Matyjaszewski, K. *Adv. Mater.* **1998**, *10*, 901.
(16) Matyjaszewski, K.; Xia, J. *Chem. Rev.* **2001**, *101*, 2921.
(17) Shipp, D. A.; Matyjaszewski, K. *Macromolecules* **2000**, *33*, 1553.
(18) Matyjaszewski, K.; Patten, T. E.; Xia, J. *J. Am. Chem. Soc.* **1997**, *119*, 674.
(19) Fischer, H. *J. Polym. Sci., Part A: Polym. Chem.* **1999**, *37*, 1885.
(20) Snijder, A.; Klumperman, B.; van der Linde, R. Submitted to *Macromolecules.*
(21) Haddleton, D. M.; Crossman, M. C.; Dana, B. H.; Duncalf, D. J.; Heming, A. M.; Kukulj, D.; Shooter, A. J. *Macromolecules* **1999**, *32*, 2110.
(22) Wang, J. L.; Grimaud, T.; Matyjaszewski, K. *Macromolecules* **1997**, *30*, 6507.
(23) Davis, K. A.; Paik, H. J.; Matyjaszewski, K. *Macromolecules* **1999**, *32*, 1767.
(24) Percec, V.; Barboiu, B.; Kim, H. J. *J. Am. Chem. Soc.* **1998**, *120*, 305.
(25) Pascual, S.; Coutin, B.; Tardi, M.; Polton, A.; Vairon, J. P. *Macromolecules* **1999**, *32*, 1432.
(26) Zhang, H.; Klumperman, B.; Ming, W.; Fischer, H.; van der Linde, R. *Macromolecules* **2001**, *34*, 6169.
(27) The numbers in the parentheses behind Ar−H and Ar−C refer to the positions of the hydrogen and carbon atoms on the anthracene group according to the IUPAC systematic nomenclature.
(28) Although the $M_{n,SEC}$ of the anthracene-containing PMMAs were not determined with PMMA standards and only were recalculated using the universal calibration principle and Mark−Houwink parameters (PS: $K = 1.14 \times 10^{-4}$ dL g^{-1}, $a = 0.716$; PMMA: $K = 0.944 \times 10^{-4}$ dL g^{-1}, $a = 0.719$), they are in good accordance with those determined by ^{1}H NMR and UV−vis methods (Table 1).
(29) Bagdasar'ian, Kh. S.; Sinitsina, Z. A. *J. Polym. Sci.* **1961**, *52*, 31.
(30) Stolka, M. *Macromolecules* **1975**, *8*, 8.
(31) Fischer, H. *Macromolecules* **1997**, *30*, 5666.
(32) Beuermann, S.; Buback, M.; Davis, T. P.; Gilbert, R. G.; Hutchinson, R. A.; Olaj, O. F.; Russell, G. T.; Schweer, J.; van Herk, A. M. *Macromol. Chem. Phys.* **1997**, *198*, 1545.
(33) Paik, H.; Matyjaszewski, K. *Polym. Prepr.* **1996**, *37*, 274.
(34) Xia, J.; Matyjaszewski, K. *Polym. Prepr.* **1996**, *37*, 513.
(35) Queffelec, J.; Gaynor, S. G.; Matyjaszewski, K. *Macromolecules* **2000**, *33*, 8629.
(36) Souaille, M.; Fischer, H. *Macromolecules* **2002**, *35*, 248.
(37) Yu, Q.; Zeng, F.; Zhu, S. *Macromolecules* **2001**, *34*, 1612.
(38) Haddleton, D. M.; Kukulj, D.; Duncalf, D. J.; Heming, A. M.; Shooter, A. J. *Macromolecules* **1998**, *31*, 5201.

MA011575Z